Temperature and heat flux of HPLC6 solution near serrated ice surfaces in unidirectional freezing

Yoshimichi Hagiwara*, Daichi Yamamoto
Department of Mechanical and System Engineering, Graduate School of Science and Technology, Kyoto Institute of Technology, Matsugasaki, Sakyo-ku, Kyoto 606-8585, Japan
*Corresponding author (E-mail: yoshi@kit.ac.jp)

1. Introduction

The inhibition of ice crystal growth is important in many fields, including cryosurgery [1], the storage of organs for transplantation [2], and lowering the energy costs associated with freezing and thawing foods. The use of ice-binding proteins is one of the most promising methods for inhibiting ice crystal growth.

One of the ice-binding proteins is HPLC6, which is extracted from winter flounder. In the experiments using a Clifton nanoliter osmometers [3], this protein is found to lower the hysteresis freezing point (HFP), while it does not alter the melting point (MP). The typical cooling rate in the osmometers was –1°C/min. In addition, the thermal hysteresis (TH), defined by the difference between MP and HFP, increases as the protein concentration increases.

Although TH is useful for the control of ice crystal growth, the gradual freezing which occurs in the osmometers differs from actual freezing in fish and in the aforementioned applications (such as cryosurgery) as follows: In the case of cryosurgery, a typical cooling rate is –10°C/min. In the case of flounder, seawater with ice crystals is taken in through the flounder's mouth, then some of the seawater flows between the gills in the capillary vessels and the remainder is ingested into the intestinal tract [4]. The blood and intestinal tract are cooled quickly by the seawater.

Our research group conducted experiments on the unidirectional freezing of HPLC6 solutions of 20 mm^3 in a narrow gap (0.02 mm) between two cover glasses [5]. Capillary vessels or the membrane of intestinal tract of a winter flounder was modeled by this narrow gap. The heat flux for solidification in our experiments was at least 15 times higher than that in the osmometers. We measured liquid temperatures in a small area of 0.0010mm^2 near the serrated interfaces through near-infrared (NIR) spectroscopy. However, the temperature field and thus the local heat flux have not yet been clarified, since the measurement was made only over the small area.

In this study, we measure the temperature distribution of the same HPLC6 solution filled in the same gap as in our previous study by using an NIR camera. In addition, we estimate the concentration of HPLC6 using fluorescence microscopy. We discuss the relationship between the local concentration and the local heat flux. The sustaining mechanism of the serrated interface is also discussed.

2. Experimental methods

The apparatus consisted of an inverted microscope, NIR camera, digital multi-meter, pulse generator and bench-top cooling section. The apparatus was placed in a temperature-controlled room, kept at 8°C. The observation area was 0.43 × 0.34mm^2. The HPLC6 solution was kept in a space of 50 × 20 × 0.020mm^3 between two cover glasses. These cover glasses were cooled by an electric cooling device with coolant flowing through the device. The protein concentration was 0.25mg/ml (0.080mM). The velocity of ice growth was set at 6.0μm/s.

The use of NIR light to measure temperature is based on the principle that the absorbance spectrum of liquid depends on temperature [5]. In our experiment, the temperature was estimated from the measured absorbance of NIR light at a wavelength of 1921nm and the calibration curve between the absorbance and temperature measured with a thermocouple. The standard deviation of the discrepancy between the estimated temperature in regions near the thermocouple and the measured temperature was 0.013°C.

We utilized fluorescence microscopy to measure the local concentration of HPLC6. For this purpose, the amino-base side chain of lysine residue and that of the N-terminus in HPLC6 were tagged with fluorescein isothiocyanate (FITC). This tagging of the FITC increases the molecular weight of HPLC6 by 24%.

3. Results and discussion

3.1. In the case of pure water

It was found that the measured temperatures in the ice region are nearly the same as those predicted from the Neumann solution for unsteady one-dimensional heat conduction problem with solidification. The measured temperatures in the water region were slightly higher than the predicted temperature.

The conduction heat flux in the water region close to the interface was calculated by multiplying the thermal conductivity of water at 0°C and the temperature gradient in the region. The temperature gradient was obtained from the temperature distribution. Similarly, the conduction heat flux in the ice close to the interface was calculated by multiplying the thermal conductivity of ice at 0°C and the temperature gradient in the region. The sum of conduction heat flux in the water close to the interface and the heat flux for solidification is equal to the conduction heat flux in the ice close to the interface, with a discrepancy of 0.2%. It is therefore confirmed that unidirectional freezing occurs near the interface.

3.2. Temperature distribution near the ice/solution interface

Figure 1 shows a typical image with the interface in the case of HPLC6 solution. The bold black lines are the wires of the thermocouple. The ice grew in the X-direction. Two points (*F* and *F'*) are the front edges of the interface, while the two other points are the bottom edges. Since the temperature at the front edge is higher than that at the bottom edge [5], we distinguished the temperature in a narrow region including the front edge (labeled *front edge*) from that in a narrow region including the bottom edge (labeled *bottom edge*).

Figure 2 indicates typical temperature profiles close to the interface in the *front edge* region and *bottom edge* region. The origin of the horizontal axis x is at the edge of an image captured by the NIR camera. The dots with circles indicate the temperature of small regions including the ice/solution interface. The temperatures of sub-zero degrees in the ice region (on the left-hand side of the graph) in each figure increase with x. The temperatures in the solution region (on the right-hand side of the graph) in each figure also increase with x. The temperature near the bottom edge is lower than that near the front edge.

3.3. Heat flux near the ice/solution interface

The conduction heat flux in the solution region close to the interface was calculated by multiplying the thermal conductivity of water at 0°C and the temperature gradient in the region. The conduction heat flux close to the interface was 0.14kW/m^2 in the *front edge* region and 0.70kW/m^2 in the *bottom edge* region.

The conduction heat flux in the ice region near the interface was calculated in the same way as that in the case of the ice/water interface mentioned above. The ensemble-averaged value of the conduction heat flux in the ice close to the interface was 1.8kW/m^2 in the *front edge* region and 1.5kW/m^2 in the *bottom edge* region.

The sum of the conduction heat flux in the solution close to the interface and the heat flux for solidification is 8.2% lower than the conduction heat flux for the ice for the *front edge* region. On the other hand, the sum is approximately 32% higher than the conduction heat flux in the ice for the *bottom edge* region.

To understand this imbalance in the heat fluxes in the *bottom edge* region, we focused on the heat flux and temperature distribution in the Y-direction. Figure 3 displays the temperature distributions in the Y-direction in three small areas (*b1*, *b2* and *b3*) shown in Fig. 1. The origin of the horizontal axis (y) in this figure is located at the centre of the areas. Arrows in the figure indicate the approximate position of the interface. The distributions of the *b1* and *b2* areas have plateaus in the middle and drop sharply near the interface, with the temperature seeming to reach 0°C or sub-zero degrees at the interface. On the other hand, the temperature seems to decrease in a linear way from the center to the interface in the *b3* area, falling to 0°C at the interface. These temperature distributions are different from the nearly uniform distribution in the Y-direction in the *front edge* region. We calculated the heat flux in the Y-direction from the gradients of temperature distributions. The heat flux was 1.4kW/m^2 in the *b2* area and 1.3kW/m^2 in *b3* area. These high heat fluxes are the reason for the imbalance of heat fluxes in the X-direction mentioned above.

A heat-flux vector can be drawn from the heat fluxes in the X and Y directions. The direction of the heat-flux vector was 117° from the X-axis for the *b2* area and 119° for the *b3* area. The direction of a vector perpendicular to the ice surface is 135° from the X-axis. Thus, the heat-flux vectors are not parallel to the vector perpendicular to the interface. To understand the difference in the directions, we examined images obtained in fluorescence microscopy. Figure 4 shows the contour maps of protein concentration near the bottom edge of the serrated interface at two instants. Red areas indicate where the protein concentration is high, while blue areas indicate where the protein concentration is low. From these images, it is clear that the concentration of HPLC6 close to the interface at the bottom edge increased with time.

The concentrated protein carries thermal energy along the ice surface. This heat transfer owing to HPLC6 leads to an apparent increase in the conduction heat flux in the *bottom edge* region mentioned above. The sum of the vector of heat flux due to the concentrated protein and the vector of conduction heat flux might be perpendicular to the interface. Furthermore, the thermal energy carried by the concentrated protein is used not for the conduction in the ice but for the maintenance of a long, narrow liquid region in the ice of the *bottom*

edge region. This is the reason for the low heat flux in the ice for the *bottom edge* region mentioned above. Therefore, the two-dimensional conduction and the heat transfer due to HPLC6 are possibly the primary mechanisms for maintaining the serrated interface in non-equilibrium unidirectional freezing. These mechanisms might be related to the antifreeze activity of HPLC6.

Acknowledgments

The authors acknowledge the financial support of the Ministry of Education, Culture, Sports, Science and Technology of Japan through the Grant-in-Aid for Scientific Research (B) (No. 21360097).

References

[1] G.L. Fletcher, S.V. Goddard, Y. Wu, *CHEMTECH*, **29** (1999), 17 – 28.
[2] G. Amir et al., *J. Heart and Lung Transplantation*, **24** (2005), 1915 – 1929.
[3] H. Chao et al., *Biochemistry* **36** (1997), 14652 – 14660.
[4] P.W. Wilson et al., *J. Biological Chemistry*, **285** (2010), 34741 – 34745.
[5] Y. Hagiwara, R. Sakurai, R. Nakanishi, *J. Crystal Growth*, **312** (2010), 314 – 322.

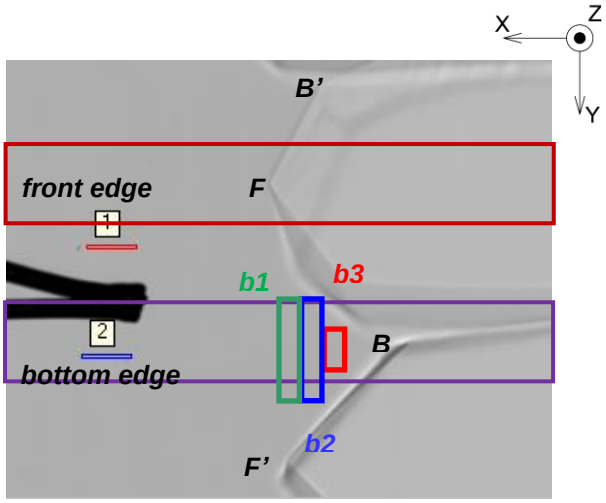

Fig.1 A typical image with an ice/solution interface

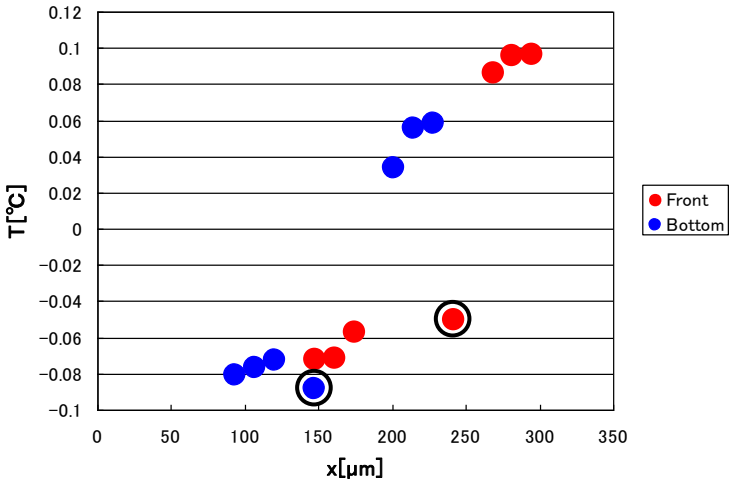

Fig.2 Temperature profiles near the ice/solution interface

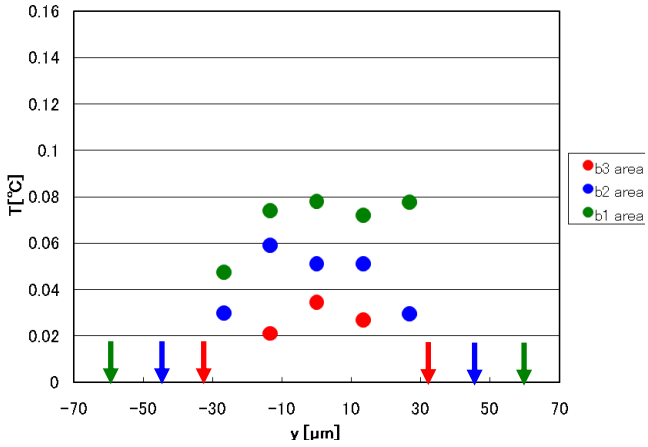

Fig.3 Temperature distributions in the Y-direction

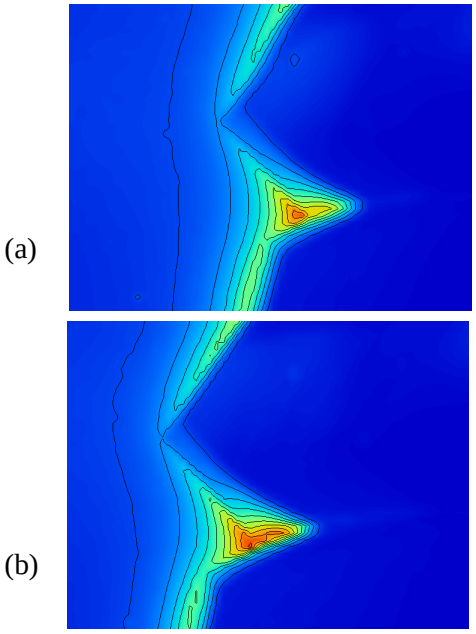

Fig.4 Contour maps of HPLC6 concentration near the bottom edge of serrated interface: (a) t, (b) t+14s